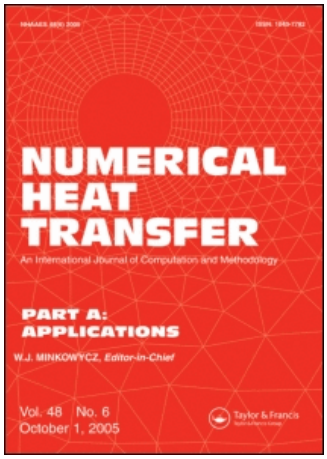

Numerical Heat Transfer, Part A: Applications
An International Journal of Computation and Methodology
Publication details, including instructions for authors and subscription information:
http://www.informaworld.com/smpp/title~content=t713657973

Effect of Length and Inclination of a Thin Fin on Natural Convection in a Square Enclosure

Abdullatif Ben-Nakhi [a]; Ali J. Chamkha [b]
[a] College of Technological Studies, The Public Authority for Applied Education and Training, Kuwait
[b] Manufacturing Engineering Department, The Public Authority for Applied Education and Training, Shuweikh, Kuwait

Online Publication Date: 01 May 2006
To cite this Article: Ben-Nakhi, Abdullatif and Chamkha, Ali J. (2006) 'Effect of Length and Inclination of a Thin Fin on Natural Convection in a Square Enclosure', Numerical Heat Transfer, Part A: Applications, 50:4, 389 - 407
To link to this article: DOI: 10.1080/10407780600619907
URL: http://dx.doi.org/10.1080/10407780600619907

Numerical Heat Transfer, Part A, 50: 389–407, 2006

ISSN: 1040-7782 print/1521-0634 online
DOI: 10.1080/10407780600619907

EFFECT OF LENGTH AND INCLINATION OF A THIN FIN ON NATURAL CONVECTION IN A SQUARE ENCLOSURE

Abdullatif Ben-Nakhi
College of Technological Studies, The Public Authority for Applied Education and Training, Kuwait

Ali J. Chamkha
Manufacturing Engineering Department, The Public Authority for Applied Education and Training, Shuweikh, Kuwait

A numerical investigation of steady, laminar, natural convective fluid flow in a square enclosure with an inclined heated thin fin of arbitrary length attached to the hot wall is considered. A transverse temperature gradient is applied on two opposing walls of the enclosure, while the other two walls are adiabatic. Attachment of highly conductive inclined thin fins with lengths equal to 20%, 35%, and 50% of the side, positioned in the middle of the hot left wall of the enclosure, is examined. The problem is formulated in terms of the vorticity–stream function procedure. A numerical solution based on the finite-volume method is obtained. Representative results illustrating the effects of the thin-fin inclination angle and length on the streamlines and temperature contours within the enclosure are reported. In addition, results for the local and average Nusselt numbers at the heated wall of the enclosure are presented and discussed for various parametric conditions. It is found that the Rayleigh number and the thin-fin inclination angle and length have significant effects on the average Nusselt number of the heated wall including the fin of the enclosure.

INTRODUCTION

The study of natural convection from finned surfaces has been the subject of many experimental and numerical investigations. This is due to the fact that the presence of a fin or array of fins on a surface may enhance the rate of heat transfer, which is very desirable in many practical applications. These investigations have been recently motivated by advances in the electronics technology and the need for efficient cooling techniques. The extent of usefulness of the increased heat transfer due to the presence of a fin or array of fins depends greatly on the proper location, size, and design of these fins on the surface. Starner and McManus [1] presented natural-convection data for four different rectangular fin arrays attached to a horizontal, a vertical, and an inclined plate. A similar experimental study was carried out by Welling and Wooldridge [2]. They reported optimum values of fin height to spacing for maximum heat transfer from rectangular fin arrays. The flow pattern

Received 24 May 2005; accepted 5 January 2006.
Address correspondence to Abdullatif Ben-Nakhi, Mechanical Power & Refrigeration Department, P.O. Box 3665, Salmiya 22037, Kuwait. E-mail: abdnakhi@yahoo.com

NOMENCLATURE

g	gravitational acceleration	v	y component of velocity
H	enclosure height	V	dimensionless Y component of velocity ($=vW/\alpha$)
l	fin length		
L	dimensionless fin length ($=l/W$)	W	enclosure width
n	distance normal to s axis	x	distance along insulated walls
N	dimensionless n coordinate ($=n/W$)	X	dimensionless distance along insulated walls ($=x/W$)
$\overline{\mathrm{Nu}}$	average Nusselt number at heated surfaces	y	distance normal to insulated walls
Nu_H	local Nusselt number at heated surfaces	Y	dimensionless distance normal to insulated walls ($=y/W$)
Pr	Prandtl number ($=\nu/\alpha$)	α	thermal diffusivity
Ra	thermal Rayleigh number $[=g\beta_T(T_h - T_c)W^3/\alpha\nu]$	β_T	thermal expansion coefficient
		ε	thin-fin inclination angle
s	coordinate adopted for distance along enclosure surfaces	ζ	dimensionless vorticity ($\Omega W^2/\alpha$)
		θ	dimensionless temperature $[=(T - T_c)/(T_h - T_c)]$
S	dimensionless coordinate ($=s/W$)		
T	temperature	ν	kinematic viscosity
T_c	cold wall temperature (sink)	ρ	density
T_h	hot surfaces temperature (source)	ψ	dimensionless stream function ($=\Psi/\alpha$)
u	x component of velocity	Ψ	stream function
U	dimensionless X component of velocity ($=uW/\alpha$)	Ω	vorticity
		∇^2	Laplacian operator

associated with free-convection heat transfer from horizontal fin arrays has also been investigated by Harahap and McManus [3].

Natural-convection heat transfer in square, rectangular, inclined, slender, and shallow cavities with various wall conditions has been extensively considered in the open literature. Owing the many possible practical applications, modification of heat transfer in cavities due to the presence of fins attached to the walls has received some consideration in recent years. Some of these applications can be found in solar collectors, nuclear reactors, heat exchangers, and electronic equipment. Upon proper placing of the fins on the walls of an enclosure, the heat transfer rate through the enclosure may be enhanced or reduced. Oosthuizen and Paul [4] considered free-convection heat transfer in a cavity fitted with a horizontal plate on the cold wall. Shakerin et al. [5] considered natural convection in an enclosure with discrete roughness elements on a vertical heated wall. Frederick [6] analyzed natural convection in an inclined square enclosure with a partition attached to its cold wall. Frederick and Valencia [7] studied the heat transfer in a square cavity with a conducting partition on its hot wall. Nag et al. [8] considered natural convection in a differentially heated square cavity with a horizontal partition plate on the hot wall. Hasnaoui et al. [9] studied numerically a vertical, rectangular, differentially heated enclosure with adiabatic fins attached to the heated wall. The enclosure aspect ratio was from 2 to 3, the dimensionless fin length from 0 to 0.75, and the microcavity height from 0.30 to 0.67. Their study showed that the heat transfer through the cold wall was reduced compared to the case without fins, and this reduction was enhanced with increasing fin length and decreasing Rayleigh number. In a subsequent work, Hasnaoui et al.

[10] extended their previous work to the inclined tall enclosure case with an enclosure aspect ratio from 2.5 and higher, dimensionless fin length from 0 to 1, with microcavity height from 0.25 to 2. The Rayleigh number was from 10^4 to 2×10^5. Hasnaoui et al. found, among other things, that the fin length was an important parameter. Specifically, at low Rayleigh numbers, the heat transfer was reduced with increasing fin length, but at high Rayleigh numbers there was an optimum value. Scozia and Frederick [11] considered natural-convection heat transfer in a differentially heated, slender rectangular cavity of aspect ratio 20 with multiple conducting fins attached on the active cold wall of the cavity. They concluded that as the interfin aspect ratio was varied from 20 to 0.25, the flow patterns evolved considerably and the average Nusselt number exhibited maximum and minimum values whose locations depended the value of the Rayleigh number. Facas [12] studied natural convection in a slender cavity of aspect ratio 15 with fins attached to both vertical, differentially heated walls. For small fin lengths, the flow was slightly blocked and a multicellular flow structure was observed. However, for longer fin lengths, the flow was blocked further, and secondary recirculation cells were formed in addition to the primary recirculation. As a result, higher heat transfer rates across the two sides of the cavity were observed. Lakhal et al. [13] considered natural convection in inclined rectangular enclosures of aspect ratios 2.5 or higher with perfectly conducting fins attached on the heated wall. They have concluded that the flow regime at low Rayleigh number is one of pure conduction, and the heat losses through the cold wall can be reduced considerably by using fins attached on the heated wall. Bilgen [14] studied natural convection in enclosures with partial partitions. Shi and Khodadadi [15] reported a detailed parametric study of flow and heat transfer in a lid-driven cavity with the presence of a thin fin. They showed that for high Rayleigh numbers the flow field is enhanced regardless of the fin's length and position, indicating that the extra heating mechanism outweighs the blockage effect for high Rayleigh numbers. Shi and Khodadadi [15] also reported that attaching a thin fin to the middle of the hot wall has the most remarkable effect on the fluid flow in the cavity. Furthermore, due to the presence of a thin fin, the heat transfer capacity on the anchoring wall is always degraded, however heat transfer on the cold wall without the fin can be promoted for high Rayleigh numbers and with the fins placed closer to the insulated walls.

The objective of this work is to study the effects of a heated thin-fin length and inclination angle on steady, laminar, two-dimensional, natural-convection fluid flow inside a differentially heated square enclosure. The heated inclined thin fin of arbitrary length is assumed to be attached to the middle of the heated wall of the enclosure, as this was shown by Shi and Khodadadi [15] to have significant effect on the fluid movement and thus the heat transfer features.

MATHEMATICAL MODEL

Consider steady, laminar, two-dimensional, natural convection inside a square enclosure in the presence of a heated inclined thin fin of arbitrary length l attached in the middle of the hot wall. Temperatures T_h and T_c are uniformly imposed on two opposing walls such that $T_h > T_c$, while the other two walls are assumed to be adiabatic. The fin is assumed to be made of highly conductive materials and is

maintained at the same temperature as that of the hot wall to which it is attached. The width of the fin is assumed to be very small compared to the computational grid size [15]. Figure 1 shows the schematic and coordinate system of the problem under consideration. As done by Shi and Khodadadi [15], a special coordinate system (s) along the walls is adopted with its origin at $x = 0$ and $y = H$, as identified by dotted lines in Figure 1. In this figure, ε is the thin-fin inclination or tilting angle. The fluid is assumed to be incompressible, viscous, and Newtonian, having constant thermophysical properties.

The governing equations for this problem are based on the balance laws of mass, linear momentum, and energy. Taking into account the assumptions mentioned above, and applying the Boussinesq approximation for the body-force terms in the momentum equations, the governing equations can be written in dimensionless vorticity–stream function formulation as

$$\zeta = \frac{\partial V}{\partial X} - \frac{\partial U}{\partial Y} = -\nabla^2 \psi \tag{1}$$

$$U\frac{\partial \zeta}{\partial X} + V\frac{\partial \zeta}{\partial Y} = \mathrm{Pr}\,\nabla^2 \zeta + \mathrm{Ra}\,\mathrm{Pr}\left(\frac{\partial \theta}{\partial X}\right) \tag{2}$$

$$U\frac{\partial \theta}{\partial X} + V\frac{\partial \theta}{\partial Y} = \nabla^2 \theta \tag{3}$$

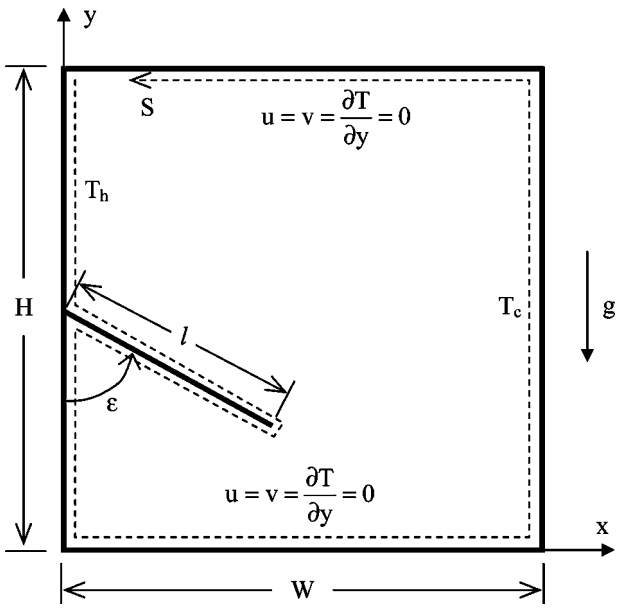

Figure 1. Schematic diagram and coordinate system for a square enclosure with inclined fin.

The boundary conditions in dimensionless form can be written as

$Y = 0$:

$$U = V = \psi = 0 \qquad \zeta = -\left(\frac{\partial^2 \psi}{\partial Y^2}\right) \qquad \frac{\partial \theta}{\partial Y} = 0 \tag{4a}$$

$Y = 1$:

$$U = V = \psi = 0 \qquad \zeta = -\left(\frac{\partial^2 \psi}{\partial Y^2}\right) \qquad \frac{\partial \theta}{\partial Y} = 0 \tag{4b}$$

$X = 0$:

$$U = V = \psi = 0 \qquad \zeta = -\left(\frac{\partial^2 \psi}{\partial X^2}\right) \qquad \theta = 1.0 \tag{4c}$$

$X = 1$:

$$U = V = \psi = 0 \qquad \zeta = -\left(\frac{\partial^2 \psi}{\partial X^2}\right) \qquad \theta = 0 \tag{4d}$$

On the fin:

$$U = V = \psi = 0 \qquad \theta = 1.0 \tag{4e}$$

In writing Eqs. (1)–(4), the following dimensionless parameters and definitions are used

$$\begin{gathered} X = \frac{x}{W} \qquad Y = \frac{y}{W} \qquad \zeta = \frac{\Omega W^2}{\alpha} \qquad \psi = \frac{\Psi}{\alpha} \qquad \theta = \frac{(T - T_c)}{(T_h - T_c)} \\ \mathrm{Pr} = \frac{\nu}{\alpha} \qquad \mathrm{Ra} = \frac{g\beta_T (T_h - T_c) W^3}{\alpha \nu} \qquad u = \frac{\partial \Psi}{\partial y} \qquad v = -\frac{\partial \Psi}{\partial x} \\ \Omega = -\left(\frac{\partial^2 \Psi}{\partial x^2} + \frac{\partial^2 \Psi}{\partial y^2}\right) \end{gathered} \tag{5}$$

All parameters appearing in the above equations are given in the Nomenclature.

The local and average Nusselt numbers at the heated wall of the enclosure including both sides of the fin are given respectively by

$$\mathrm{Nu}_H = -\left.\frac{\partial \theta}{\partial N}\right|_{N=0} \tag{6}$$

$$\overline{\mathrm{Nu}} = \frac{1}{1+2L}\int_0^{1+2L} \mathrm{Nu}_H \, dS \tag{7}$$

Similar expressions can be defined at the cooled wall of the enclosure if needed.

NUMERICAL ALGORITHM

The governing Eqs. (1)–(3) for laminar, two-dimensional, natural-convection heat transfer in a square enclosure with an inclined thin fin are solved using the Gauss-Seidel point-by-point method as discussed by Patankar [16], along with underrelaxation factors for temperature, vorticity, and stream functions. For the numerically unstable cases, steady-state solutions were obtained by employing transient formulation of the governing equations. The convergence criterion employed to reach the steady-state solution was the standard relative error, which is based on the maximum norm given by

$$\Delta = \frac{\left\|\zeta^{m+1} - \zeta^{m}\right\|_\infty}{\left\|\zeta^{m+1}\right\|_\infty} + \frac{\left\|\theta^{m+1} - \theta^{m}\right\|_\infty}{\left\|\theta^{m+1}\right\|_\infty} \leq 10^{-6} \tag{8}$$

where the operator $\|\eta\|_\infty$ indicates the maximum absolute value of the variable over all the grid points in the computational domain, and m and $m+1$ represent the old time and advanced time step, respectively.

An unstructured grid of triangular mesh elements was employed in the current work. A total of 11,535 nodes was used in the model. The aspect ratio and skewness of the mesh cells have significant effects on the accuracy of the numerical solution. In the current work, the mesh quality of the numerical model was analyzed by means of aspect ratio, equiangle skew, and equisize skew of each cell within the domain. The aspect ratio Q_{AR} is defined by

$$Q_{\mathrm{AR}} = 0.5\frac{R}{r} \geq 1.0 \tag{9}$$

where r and R represent the radii of the circles that inscribe and circumscribe, respectively, the mesh element. Here 90% of the cells have $1.0 \leq Q_{\mathrm{AR}} \leq 1.01$ and 99% of the cells have $1.0 \leq Q_{\mathrm{AR}} \leq 1.08$, where $Q_{\mathrm{AR}} = 1.0$ describes an equilateral element.

The equiangle skew Q_{EAS} is a normalized measure of skewness that is defined as

$$Q_{\mathrm{EAS}} = \max\left\{\frac{\theta_{\max} - 60}{120}, \frac{60 - \theta_{\min}}{60}\right\} \tag{10}$$

where $\theta_{\max}$ and $\theta_{\min}$ are the maximum and minimum angles (in degrees) between the edges of the triangular cell. Accordingly, $0.0 \leq Q_{\mathrm{EAS}} \leq 1.0$, where $Q_{\mathrm{EAS}} = 0.0$ describes an equilateral element, and $Q_{\mathrm{EAS}} = 1.0$ describes a completely degenerate (poorly shaped) element. Here 90% of the cells have $0.0 \leq Q_{\mathrm{EAS}} \leq 0.08$ and 99%

Table 1. Comparison of predicted average Nusselt number $\overline{\mathrm{Nu}}$ on the left or right wall of a differentially heated enclosure without a fin with results of [8, 15, 18, 19]

Ra	10^4	10^5	10^6
De Vahl Davis and Jones [17]	2.243	4.519	8.800
De Vahl Davis [18]	2.243	4.519	8.800
Nag et al. [8]	2.240	4.510	8.820
Shi and Khodadadi [15]	2.247	4.532	8.893
Present work	2.244	4.524	8.856

of the cells have $0.0 \leq Q_{\mathrm{EAS}} \leq 0.24$. In general, high-quality meshes contain elements that possess Q_{EAS} values not exceeding 0.25. The equisize skew Q_{ESS} is a measure of skewness that is defined as

$$Q_{\mathrm{ESS}} = \frac{S_{\mathrm{eq}} - S^*}{S_{\mathrm{eq}}} \tag{11}$$

where S^* is the area of the triangular cell and S_{eq} is the maximum area of an equilateral triangular cell the circumscribing radius of which is identical to that of the mesh element. Accordingly, $0.0 \leq Q_{\mathrm{ESS}} \leq 1.0$, where $Q_{\mathrm{ESS}} = 0.0$ describes an equilateral element, and $Q_{\mathrm{ESS}} = 1.0$ describes a completely degenerate (poorly shaped) element. Here 90% of the cells have $0.0 \leq Q_{\mathrm{EAS}} \leq 0.01$ and 99% of the cells have $0.0 \leq Q_{\mathrm{AR}} \leq 0.1$. In general, high-quality meshes contain element Q_{ESS} values of 0.1 or less. In the present work, all requirements for high-quality meshes are satisfied.

The accuracy of the numerical scheme is validated by comparing the average Nusselt number $\overline{\mathrm{Nu}}$ for a differentially heated square enclosure in the absence of the fin for various Rayleigh numbers with those reported by De Vahl Davis and Jones [17] and De Vahl Davis [18], Nag et al. [8], and Shi and Khodadadi [15]. These comparisons show excellent agreement, as shown in Table 1. In addition, further validation is performed by comparing the present results with the results of various cases of the problem of Shi and Khodadadi [15], who considered a similar configuration with a noninclined fin, and reasonable agreement is observed as is evident from Figure 2. This favorable comparison lends confidence to the numerical results presented in the next section.

RESULTS AND DISCUSSION

In this section, numerical results for the streamline and temperature contours for various values of the fin inclination angle ε and length L are reported. In addition, representative results for the local and average Nusselt numbers (Nu_H and $\overline{\mathrm{Nu}}$) at various conditions are presented and discussed.

Figures 3–5 present steady-state contour plots for the streamline and temperature for various values of the fin inclination angle for $\mathrm{Pr} = 0.707$, $\mathrm{Ra} = 10^5$, and the three different fin lengths, $L = 0.2$, 0.35, and 0.5, respectively. In the absence of the thin fin ($\varepsilon = 0^\circ$ or $\varepsilon = 180^\circ$), a clockwise-rotating vortex is formed. This is due

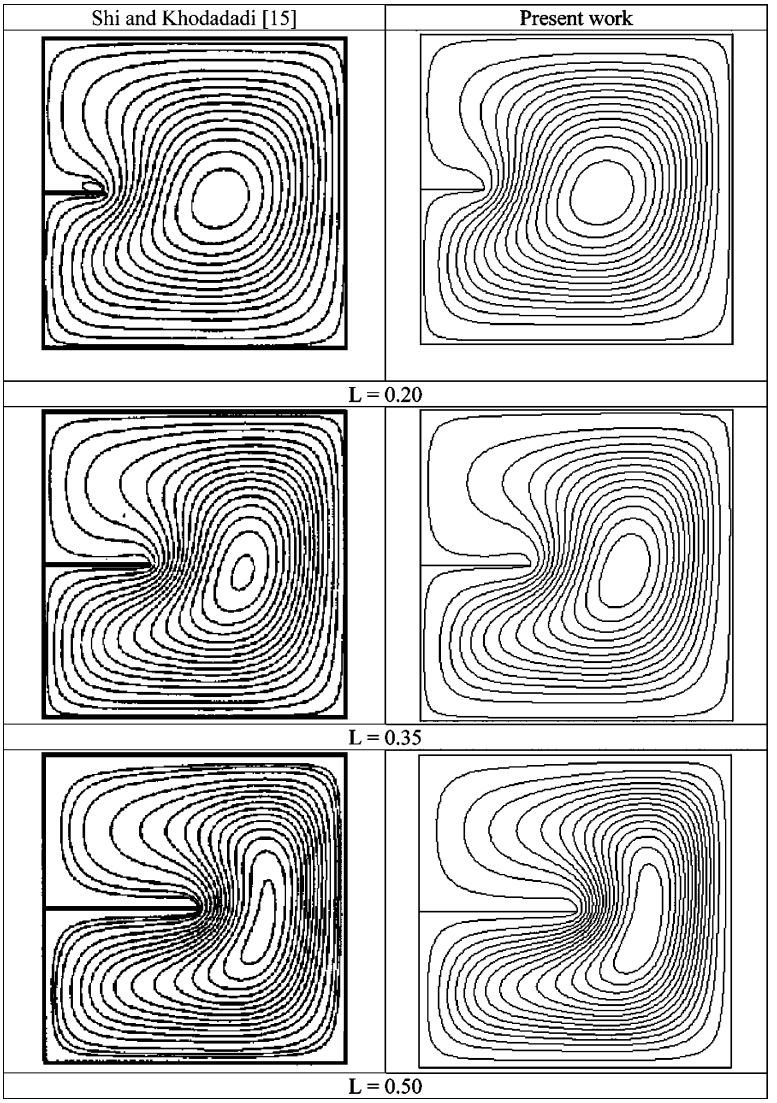

Figure 2. Comparison of stream functions with those of Shi and Khodadadi [15] for Ra = 10^4.

to the rise of the fluid due to buoyancy effects produced by heating of the left wall of the enclosure and the consequent falling of the fluid on the right cold wall. The streamline contours exhibit a feature whereby a primary recirculating cell includes two secondary cells with almost uniform horizontal temperature contours in the core region of the enclosure away from the boundaries. In general, the presence of a non-inclined fin attached to the hot wall of the enclosure tends to create a blockage to flow movement close to the hot wall, causing a weakening of the primary recirculating cell. It has been reported by Shi and Khodadadi [15] that the effect of a thin noninclined fin attached to the middle of the hot wall has the most remarkable effect

on the fluid flow in the enclosure. The presence of a thin noninclined fin attached at the middle of the hot wall redirects the movement of the fluid and weakens the fluid motion within the area above the fin. This alteration in the fluid movement within the enclosure has a direct effect on the wall heat transfer. Also, the blockage effect due to the presence of the fin depends greatly on its length. The longer the fin, the bigger the blockage effect, and therefore, the more changes there are in the flow and heat transfer characteristics.

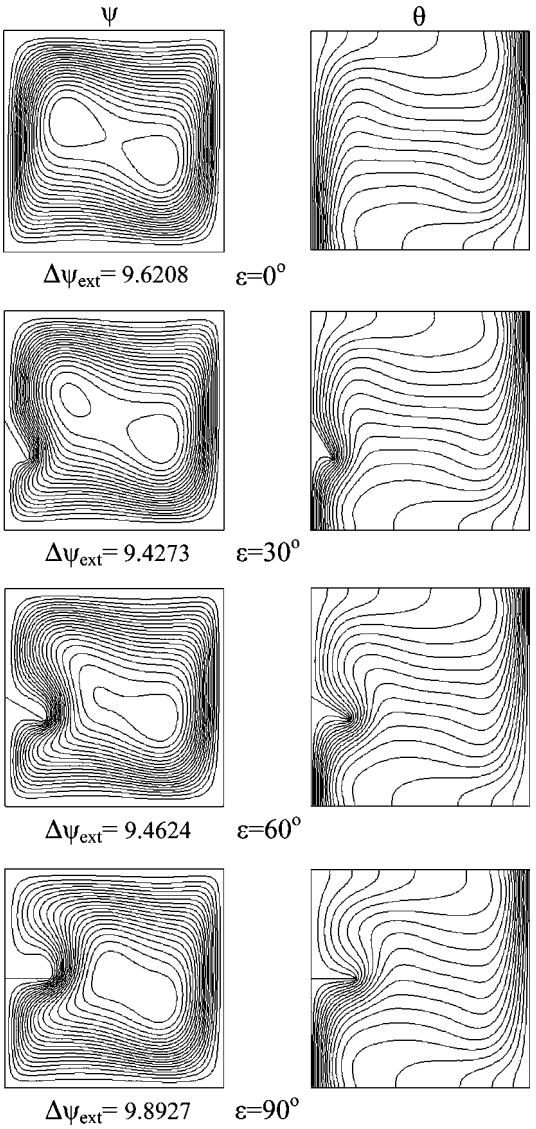

Figure 3. Effects of ε on the contour maps of the streamlines and isotherms; $\mathrm{Pr} = 0.707$, $\mathrm{Ra} = 10^5$, $L = 0.2$.

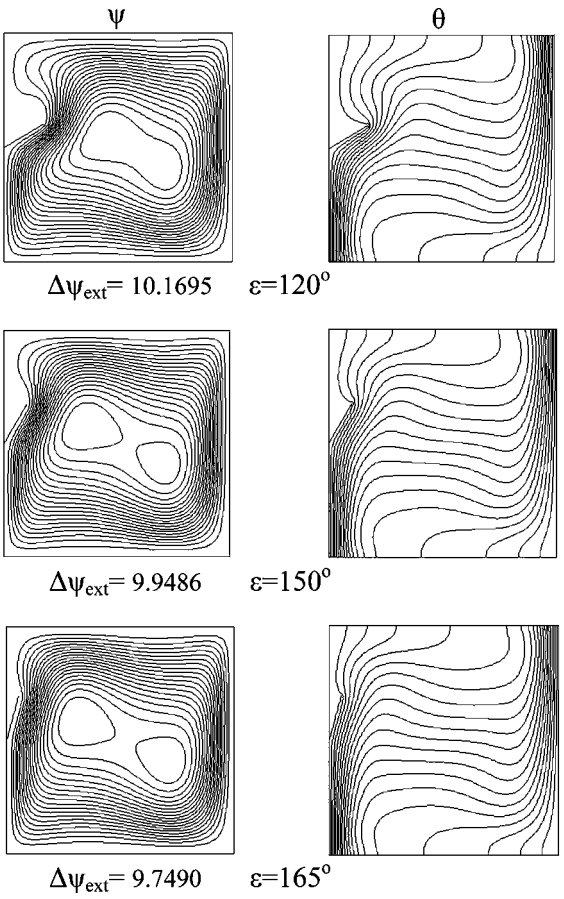

Figure 3. Continued.

In general, irregardless of the fin length, as the fin inclination angle ε increases, the flow movement below the fin is enhanced while the flow above it slows down, causing the secondary cells within the primary vortex to connect and become a part of the main cell. In general, the change of the extreme stream function values $\Delta\psi_{ext}$ tend to increase as ε is increased from 15° to 120° and then begins to decrease for $\varepsilon > 120^\circ$, where the secondary cells tend to separate again. This is true for fin lengths considered in the present study. The redirection of the flow movement within the enclosure increases as the length of the fin increases, and the most effect appears clearly when $\varepsilon = 90^\circ$. Also, for $\varepsilon = 0^\circ$ (no-fin case), the isotherms in the core region of the enclosure (away from the walls) are almost uniform and parallel to the insulating walls. However, as ε increases, the isotherms in the core region become nonlinear and the nonlinearity becomes more pronounced for $\varepsilon = 90^\circ$ and as the fin length is increased more and more. The changes in the temperature distributions within the core of the enclosure as well as close to the heated and cooled walls as either ε or L is increased bring about changes in the wall heat transfer.

Figure 6 presents the change of the extreme stream function values $\Delta\psi_{ext}$ versus the fin inclination angle ε for the three different fin lengths considered in the previous figures ($L = 0.2$, 0.35, and 0.5). It is clearly observed from this figure that the values of $\Delta\psi_{ext}$ increase significantly in the range $80^\circ < \varepsilon < 130^\circ$, whereas they decrease in the range $130^\circ < \varepsilon < 180^\circ$ as L is increased from 0.2 to 0.5. For smaller fin

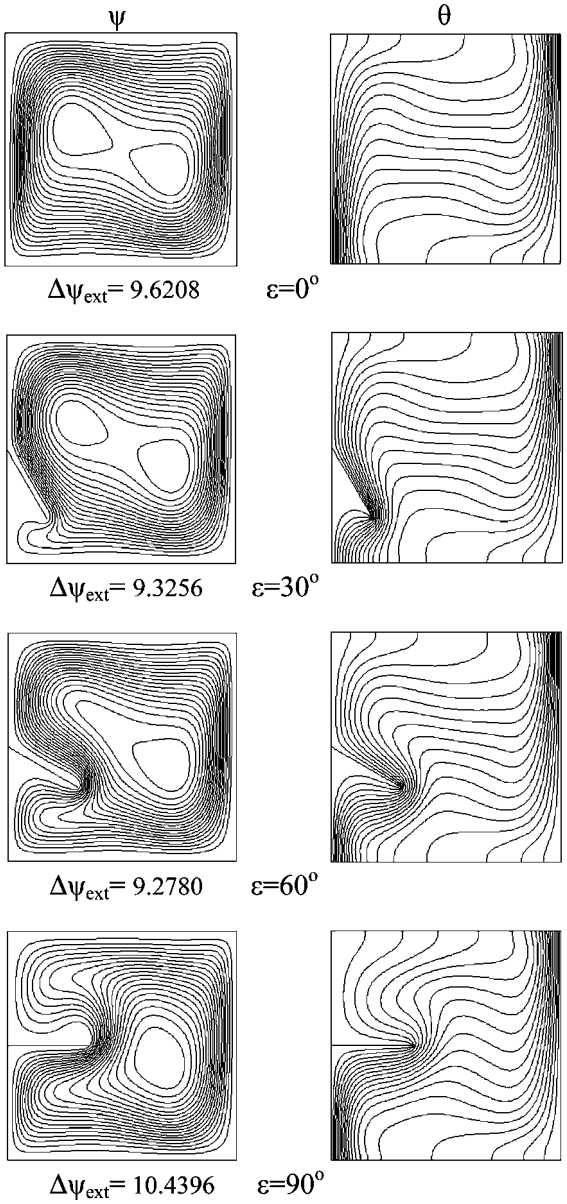

Figure 4. Effects of ε on the contour maps of the streamlines and isotherms; $Pr = 0.707$, $Ra = 10^5$, $L = 0.35$.

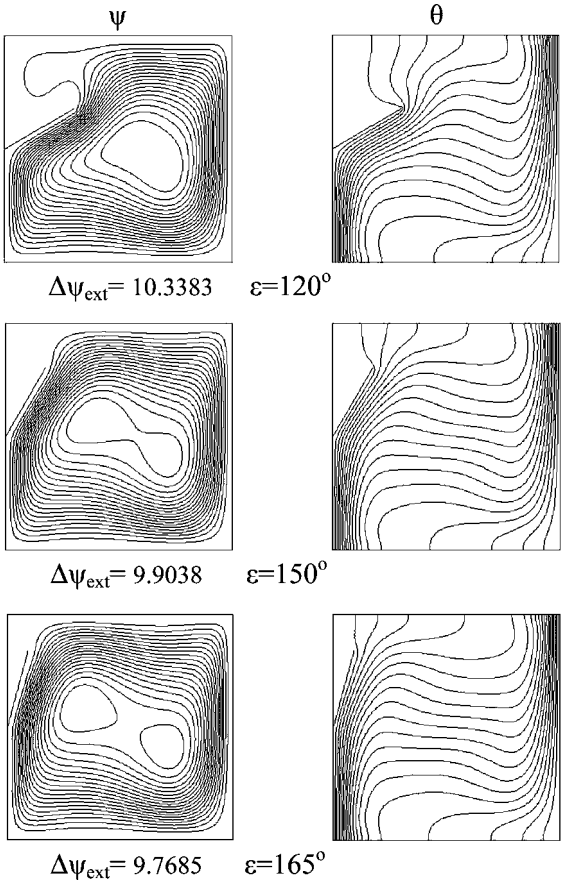

Figure 4. Continued.

inclination angles $0^\circ < \varepsilon < 70^\circ$, the values of $\Delta\psi_{ext}$ decrease as L is increased from 0.2 to 0.35. However, different behavior is predicted for $L = 0.5$, for which the values of $\Delta\psi_{ext}$ increase significantly above the values corresponding to $L = 0.2$ in the range $0^\circ < \varepsilon < 55^\circ$ and then decrease in the range $55^\circ < \varepsilon < 70^\circ$. It is also seen from this figure that for a given value of L, a distinctive peak in the value of $\Delta\psi_{ext}$ occurs at a specific fin inclination angle. For example, the peak values of $\Delta\psi_{ext}$ for $L = 0.2$, 0.35, and 0.5 occur at $\varepsilon = 120^\circ$, 103°, and 105°, respectively. It should be mentioned that for $L = 0.5$, another lower peak occurs at $\varepsilon = 32^\circ$.

Figures 7–9 illustrate the effect of the fin inclination angle ε on the local Nusselt number at the heated wall including both sides of the fin Nu_H for the three different fin lengths $L = 0.2$, 0.35, and 0.5, respectively. For clarity, the Nu_H profile for $\varepsilon = 90^\circ$ is distinguished by a thicker line, the Nu_H profiles for $\varepsilon < 90^\circ$ are designated by solid thin lines, and the Nu_H profiles for $\varepsilon > 90^\circ$ are represented by dashed thin lines. In the absence of the thin fin, the local Nusselt number increases as the dimensionless distance S increases, with a slight drop close to the lower insulated wall of the enclosure. However, in the presence of a fin, the local Nusselt number

exhibits a sharp reduction at the location of the wall/fin intersection, where it becomes a minimum due to flow stagnation. In principle, the attachment of a fin in the middle of the heated wall always reduces the local Nusselt number for the heated wall by a ratio that is related to ε and L. As mentioned before, this is due to the fact that the fin blocks the flow near the heated wall. Figures 7–9 also show

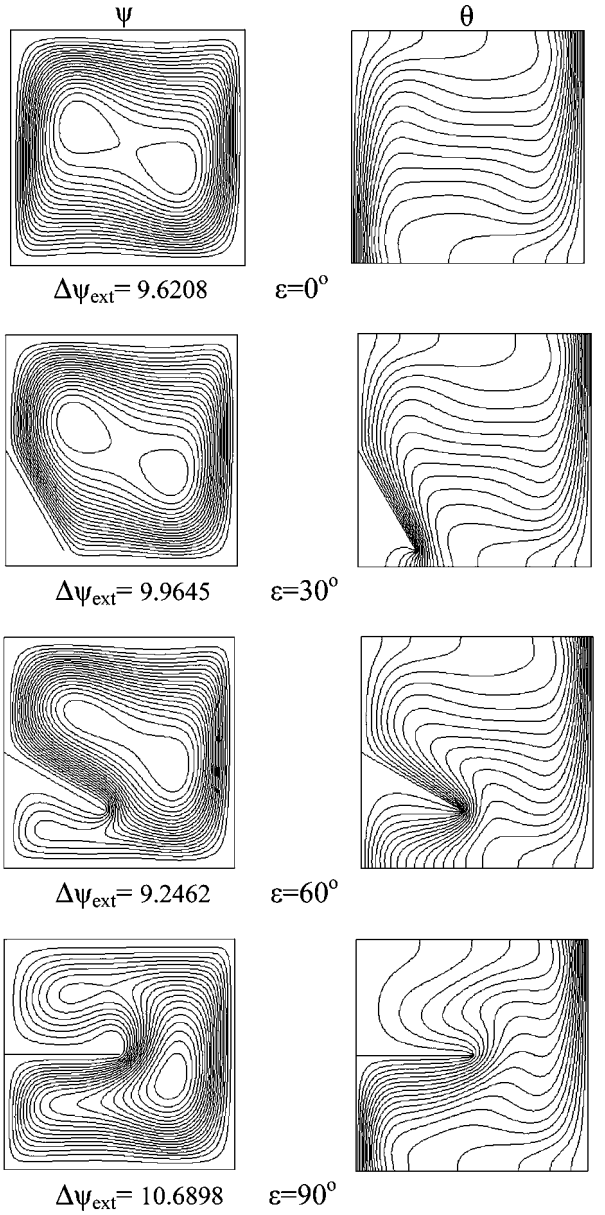

Figure 5. Effects of ε on the contour maps of the streamlines and isotherms; $\mathrm{Pr} = 0.707$, $\mathrm{Ra} = 10^5$, $L = 0.5$.

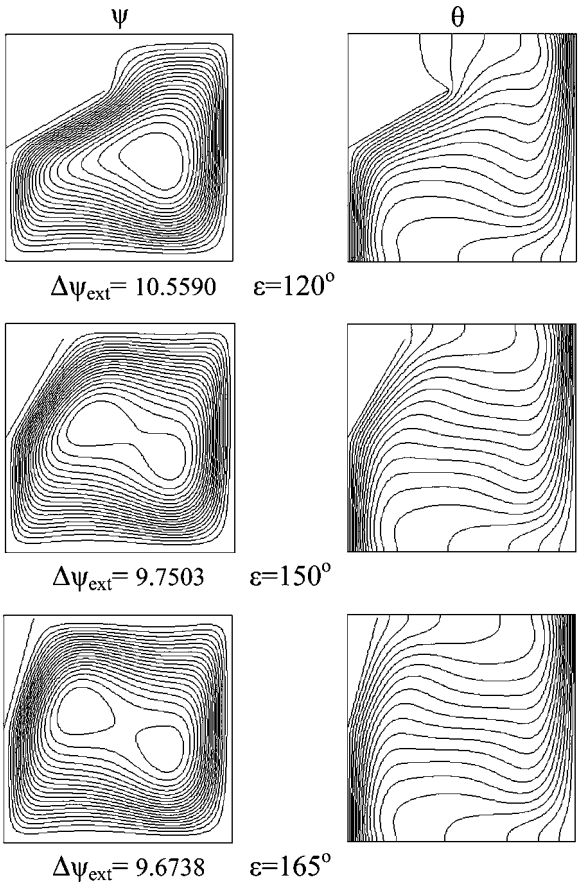

Figure 5. Continued.

that the local Nusselt number is inversely related to ε on the upper half of the heated wall, whereas it is directly related to ε on the lower half of the heated wall. The relation between the local Nusselt number and ε is more complex for the upper and lower surfaces of the fin. For the upper surface of the fin, Nu_H decreases as ε increases until the dip in the Nu_H profile is reached at $\varepsilon = 90^\circ$ for $L = 0.2$ and 0.35 or at $\varepsilon = 75^\circ$ for $L = 0.5$. For ε values greater than the corresponding angle at the dip location, the Nu_H value is directly related to ε within the area near the fin base, and inversely related within the area near the fin tip. Equivalently, for the lower surface of the fin, Nu_H increases as ε increases until the peak in the Nu_H profile is reached at $\varepsilon = 90^\circ$ for $L = 0.2$ and 0.35 or at $\varepsilon = 75^\circ$ for $L = 0.5$. For ε values greater than the corresponding angle at the peak, the Nu_H value is inversely related to ε.

Figure 10 displays the influence of the fin inclination angle ε and the fin length L on the average Nusselt number at the heated surfaces $\overline{\mathrm{Nu}}$. It is clearly observed that the fin inclination angle and length have significant effects on the average Nusselt number. In general, for a fixed value of ε other than 0° and 180°, as the

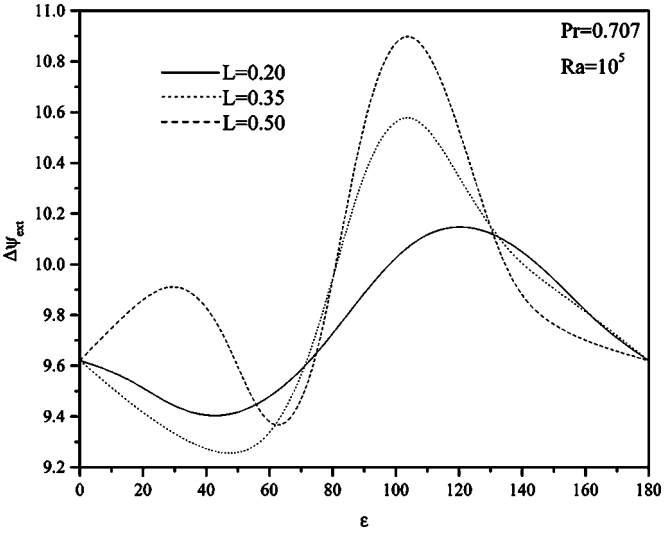

Figure 6. Effects of fin length L on $\Delta\psi_{ext}$.

fin length increases, the average Nusselt number decreases significantly. On the other hand, the average Nusselt number tends to increase appreciably, especially for shorter fins, as the fin inclination angle increases beyond a critical value which depends on the fin length. For $L = 0.2$, the critical value of ε is observed to be 105°. Below this critical value of ε, a drastic drop in terms of $\overline{Nu}$ is observed as ε increases. For relatively longer fins ($L = 0.35$ and $L = 0.5$), the values of $\overline{Nu}$ tend

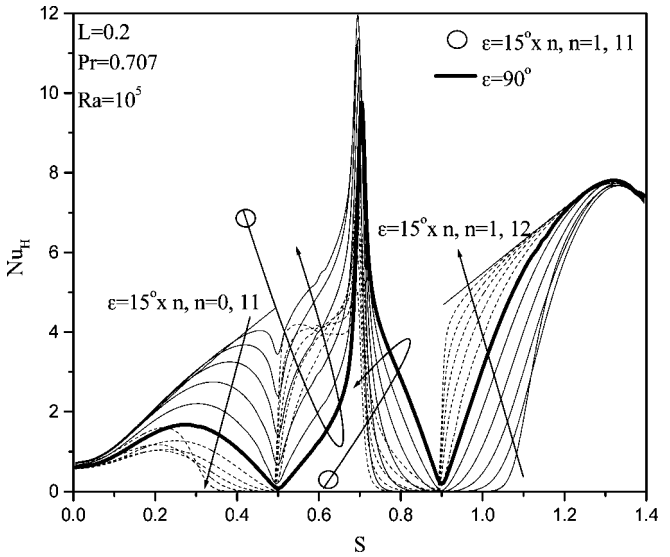

Figure 7. Effects of ε on hot wall and fin local Nusselt number for $L = 0.2$.

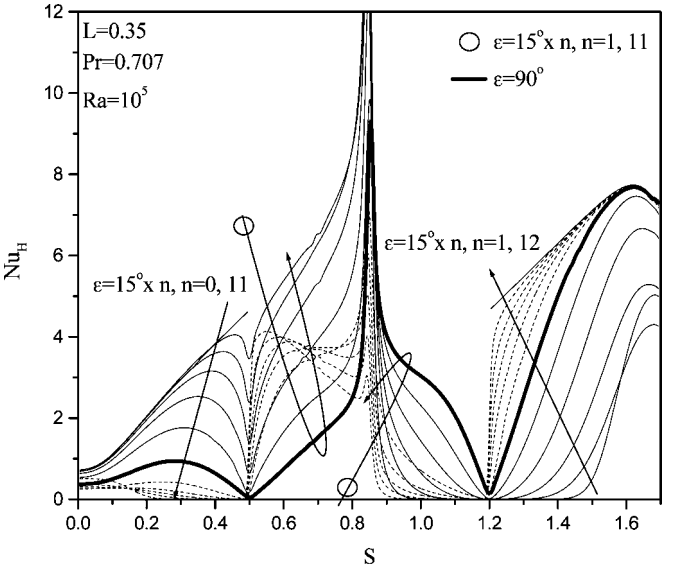

Figure 8. Effects of ε on hot wall and fin local Nusselt number for $L = 0.35$.

to decrease and then increase as ε increases. In fact, there are three critical values of ε for which $\overline{\mathrm{Nu}}$ is a relative minimum. For $L = 0.35$, these critical values of ε are 15°, 105°, and 165°, while for $L = 0.5$, the critical values of ε are 15°, 75°, and 165°.

Figure 11 presents the average Nusselt on the heated wall of the enclosure including the fin for $\varepsilon = 45°$ versus the Rayleigh number Ra for three different values

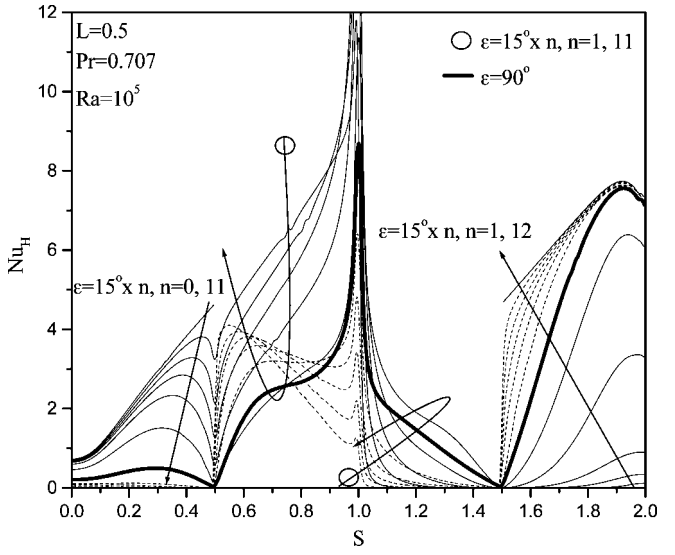

Figure 9. Effects of ε on hot wall and fin local Nusselt number for $L = 0.5$.

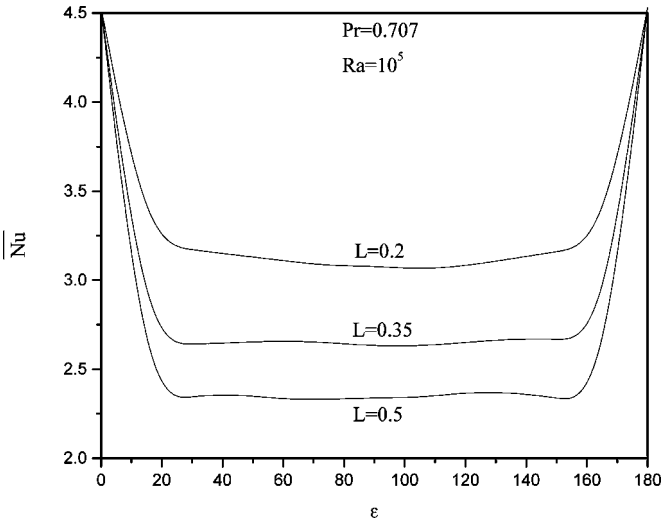

Figure 10. Effects of ε and L on hot wall and fin average Nusselt number.

of fin length L (0.2, 0.35, and 0.5). Also plotted in this figure is the case in which the fin is absent ($\varepsilon = 0^\circ$). For a fixed value L and $\varepsilon = 45^\circ$, it is observed that the average Nusselt number increases as Ra increases. By comparison of $\overline{Nu}_{,\varepsilon=45^\circ}$ with $\overline{Nu}_{,\varepsilon=0^\circ}$, it is observed that the values of $\overline{Nu}_{,\varepsilon=45^\circ}$ are lower than those corresponding to $\overline{Nu}_{,\varepsilon=0^\circ}$ regardless of the fin length. In addition, it is shown that the average Nusselt number decreases as the length of the fin is increased. This is consistent with the results in Figure 10.

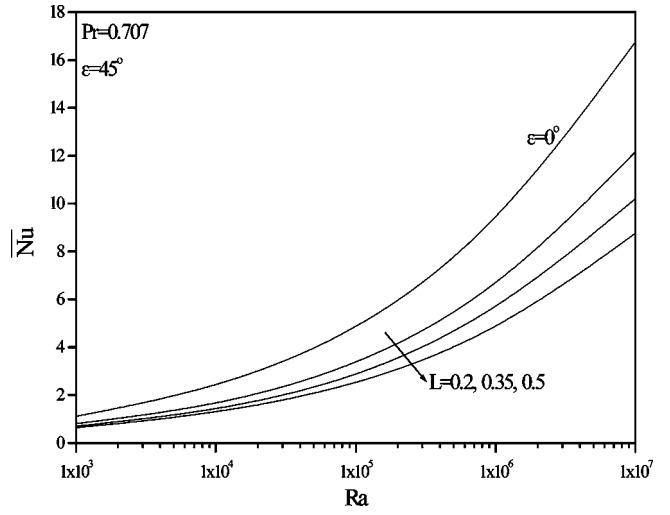

Figure 11. Effects of Ra and L on hot wall and fin average Nusselt number for $\varepsilon = 45^\circ$.

CONCLUSIONS

Natural-convection heat transfer in a differentially heated square enclosure in the presence of a heated inclined thin fin attached to the middle of the heated wall was studied numerically. The governing equations for this investigation were put in the dimensionless vorticity–stream function formulation and were solved by the finite volume technique. Graphical results for the streamline and temperature contours for various parametric conditions were presented and discussed. It was found that the thin-fin inclination angle and length had significant effects on the average Nusselt number of the heated wall of the enclosure including the fin. In general, the average Nusselt number decreased appreciably as the length of the fin was increased. On the other hand, different behavior of the average Nusselt number was predicted as the fin inclination angle was increased, depending on the thin fin length. For a small fin length, the average Nusselt number decreased as ε was increased up to a critical value, after which it increased. On the other hand, for long fins, the average Nusselt number decreased and then increased as ε was increased, resulting in three critical fin angles for which the average Nusselt number is a relative minimum. In addition, increasing the Rayleigh number produced significant increases in the average Nusselt number. In light of the predicted results, it can be concluded that in design problems, it is possible to enhance or reduce wall heat transfer by proper selection of both the fin inclination angle and length as well as the Rayleigh number.

REFERENCES

1. K. E. Starner and H. N. McManus, An Experimental Investigation of Free Convection Heat Transfer from Rectangular Fin-Arrays, *J. Heat Transfer*, vol. 85, pp. 273–278, 1963.
2. J. R. Welling and C. B. Wooldridge, Free Convection Heat Transfer Coefficient from Rectangular Vertical Fins, *J. Heat Transfer*, vol. 87, pp. 439–444, 1965.
3. F. Harahap and H. N. McManus, Natural Convection Heat Transfer from Horizontal Rectangular Fin Arrays, *J. Heat Transfer*, vol. 89, pp. 32–38, 1967.
4. P. Oosthuizen and J. T. Paul, Free Convection Heat Transfer in a Cavity Fitted with a Horizontal Plate on the Cold Wall, Advances in Enhanced Heat Transfer – 1985. Presented at the 23rd ASME National Heat Transfer Conference, vol. 43, pp. 101–107, 1985.
5. S. Shakerin, M. Bohn, and R. I. Loehrke, Natural Convection in an Enclosure with Discrete Roughness Elements on a Vertical Heated Wall, *Int. J. Heat Mass Transfer*, vol. 31, pp. 1423–1430, 1988.
6. R. L. Frederick, Natural Convection in an Inclined Square Enclosure with a Partition Attached to Its Cold Wall, *Int. J. Heat Mass Transfer*, vol. 32, pp. 87–94, 1989.
7. R. L. Frederick and A. Valencia, Heat Transfer in a Square Cavity with a Conducting Partition on Its Hot Wall, *Int. Commun. Heat Mass Transfer*, vol. 16, pp. 347–354, 1989.
8. A. Nag, A. Sarkar, and V. M. K. Sastri, Natural Convection in a Differentially Heated Square Cavity with a Horizontal Partition Plate on the Hot Wall, *Comput. Meth. Appl. Mech. Eng.*, vol. 110, pp. 143–156, 1993.
9. M. Hasnaoui, P. Vasseur, and E. Bilgen, Natural Convection in Rectangular Enclosures with Fins Attached to One of the Isothermal Walls, Solar Engineering 1990 – Presented at the Twelfth Annual International Solar Energy Conference, p. 131–137, ASME, New York, NY, USA, 1990.

10. M. Hasnaoui, P. Vasseur, and E. Bilgen, Natural Convection in Rectangular Enclosures with Adiabatic Fins Attached on the Heated Wall, *Wärme Stoffubertrag.*, vol. 27, pp. 357–368, 1992.
11. R. Scozia and R. L. Frederick, Natural Convection in Slender Cavities with Multiple Fins Attached on an Active Wall, *Numer. Heat Transfer A*, vol. 20, pp. 127–158, 1991.
12. G. N. Facas, Natural Convection in a Cavity with Fins Attached to Both Vertical Walls, *J. Thermophys. Heat Transfer*, vol. 7, pp. 555–560, 1993.
13. E. K. Lakhal, M. Hasnaoui, E. Bilgen, and P. Vasseur, Natural Convection in Inclined Rectangular Enclosures with Perfectly Conducting Fins Attached on the Heated Wall, *Heat Mass Transfer*, vol. 32, pp. 365–373, 1997.
14. E. Bilgen, Natural Convection in Enclosures with Partial Partitions, *Renewable Energy*, vol. 26, pp. 257–270, 2002.
15. X. Shi and J. M. Khodadadi, Laminar Convection Heat Transfer in a Differentially Heated Square Cavity due to a Thin Fin on the Hot Wall, *J. Heat Transfer*, vol. 125, pp. 624–634, 2003.
16. S. V. Patankar, *Numerical Heat Transfer and Fluid Flow*, Hemisphere, Washington, DC, 1980.
17. G. De Vahl Davis and L. P. Jones, Natural Convection in a Square Cavity: A Comparison Exercise, *Int. J. Numer. Meth. Fluids*, vol. 3, pp. 227–248, 1983.
18. G. De Vahl Davis, Natural Convection of Air in a Square Cavity: A Bench Mark Numerical Solution, *Int. J. Numer. Meth. Fluids*, vol. 3, pp. 249–264, 1983.